ELSEVIER

Journal of Pharmaceutical and Biomedical Analysis
28 (2002) 1149–1159

JOURNAL OF
PHARMACEUTICAL
AND BIOMEDICAL
ANALYSIS

www.elsevier.com/locate/jpba

Quantitative analysis of mannitol polymorphs. X-ray powder diffractometry—exploring preferred orientation effects

Sarra N. Campbell Roberts [a], Adrian C. Williams [a,*], Ian M. Grimsey [a], Steven W. Booth [b]

[a] *Drug Delivery Group, School of Pharmacy, University of Bradford, Bradford, West Yorkshire BD7 1DP, UK*
[b] *Merck, Sharp and Dohme Research Laboratories, Hoddesdon, Hertfordshire EN11 9BU, UK*

Received 31 October 2001; received in revised form 27 November 2001; accepted 16 December 2001

Abstract

Mannitol is a polymorphic pharmaceutical excipient, which commonly exists in three forms: alpha, beta and delta. Each polymorph has a needle-like morphology, which can give preferred orientation effects when analysed by X-ray powder diffractometry (XRPD) thus providing difficulties for quantitative XRPD assessments. The occurrence of preferred orientation may be demonstrated by sample rotation and the consequent effects on X-ray data can be minimised by reducing the particle size. Using two particle size ranges (< 125 and 125–500 μm), binary mixtures of beta and delta mannitol were prepared and the delta component was quantified. Samples were assayed in either a static or rotating sampling accessory. Rotation and reducing the particle size range to < 125 μm halved the limits of detection and quantitation to 1 and 3.6%, respectively. Numerous potential sources of assay errors were investigated; sample packing and mixing errors contributed the greatest source of variation. However, the rotation of samples for both particle size ranges reduced the majority of assay errors examined. This study shows that coupling sample rotation with a particle size reduction minimises preferred orientation effects on assay accuracy, allowing discrimination of two very similar polymorphs at around the 1% level.

Keywords: Mannitol; Polymorphism; Quantitation X-ray powder diffractometry; Particle size; Sample rotation

1. Introduction

The repercussions of polymorphic transformations with regard to drug product performance are well recognised by the pharmaceutical industry. The different internal crystal structures of a given drug (which constitute the phenomenon of polymorphism) usually exhibit different physicochemical properties [1]. These variations may manifest themselves in altered bioavailabilities and chemical stabilities, which on polymorphic transformation, could subsequently jeopardise dosage form performance. The impact of such

* Corresponding author. Tel.: +44-1274-234-756; fax: +44-1274-234-769.
E-mail address: a.c.williams@bradford.ac.uk (A.C. Williams).

0731-7085/02/$ - see front matter
PII: S0731-7085(02)00053-5

transformations, therefore, warrants quantitative control to ensure that the polymorphic composition remains within stated limits throughout the shelf-life of the drug product [2]. Similar concerns exist for pharmaceutical excipients since the various polymorphic forms may lead to different biological activities [3]. Mannitol is a common pharmaceutical excipient exhibiting at least three polymorphic forms: alpha, beta and delta, which can be found in lyophilised products such as injections and granulated powders for oral use. Mannitol is also used in chewable tablet formulations and lozenges as it imparts a cooling sensation in the mouth, has approximately half the sweetness of sucrose yet is non-cariogenic [4,5]. Each polymorphic form shows differences in physical properties such as melting point, density and compression behaviour. Transitions at elevated temperatures and solution-mediated transformations at ambient temperatures have been observed with some of the mannitol polymorphs; the transition product was identified as the most stable beta form.

Many techniques have been used to determine content in mixtures of active pharmaceutical polymorphs or amorphous content in crystalline drug. Reflectance IR spectroscopy (near- and mid-IR) was used by Patel et al. [6], Luner et al. [7] and Bugay et al. [8]. Quantitative studies of ampicillin and sulphamethoxazole indicated that levels of 1% could be predicted using near-IR reflectance spectroscopy [7]. Bugay et al. reported a limit of detection (LOD) of 0.3% (w/w) and limit of quantitation (LOQ) of 1% (w/w) for quantitation of cefepime·2HCl dihydrate in cefepime·2HCl monohydrate [8]. FT-Raman spectroscopy is increasingly being used in a quantitative capacity; Taylor and Zografi assessed proportions of crystalline and amorphous indomethacin using a ratio of peak heights unique to each component. A LOD of 0.6% and LOQ of 2% were calculated for both constituents [9]. The quantitation of mannitol using this spectroscopic technique also gave a LOQ of approximately 2% for the beta form in mixtures containing beta and delta [10]. Calcium oxalate monohydrate, a mineral component present in urinary stones was detectable at levels of 0.6 mol% according to the FT-Raman spectroscopic study completed by Kontoyannis et al. [11]. In a similar study, Kontoyannis et al. compared the quantitative data obtained for calcite, aragonite and gypsum using FT-Raman spectroscopy and powder X-ray diffractometry (PXRD) where relatively lower detection limits for each material were obtained using the spectroscopic technique [12]. Solid-state NMR spectroscopy has also been employed in quantitative applications where it offers a high degree of spectral resolution [13]. Gao successfully quantified mixtures of delavirdine mesylate polymorphs achieving a detection limit of 2–3% [14].

Despite the above, X-ray powder diffractometry (XRPD) is usually the preferred method for the analysis of polymorphic content in mixtures [1]. Chao and Vail analysed 1,2-dihydro-6-neopentyl-2-oxonicotinic acid using PXRD and reported a detection limit of less than 1% of form I in form II [15]. Similarly, the quantitation of cefepime·2HCl dihydrate in cefepime·2HCl monohydrate resulted in a detection limit of 0.75% (w/w) dihydrate and a quantitation limit of 2.5% (w/w) [8]. XRPD has also been used to quantify sample crystallinity [16,17] even though, generally, no clearly defined diffraction peaks are recorded with amorphous materials. In determining the degree of crystallinity of a leukotriene biosynthesis inhibitor, Clas et al. reported a detection limit of approximately 5–10% of the crystalline phase [16]. Surana and Suryanarayanan showed a lower detection limit of 0.9% (w/w) for crystalline sucrose in mixtures containing crystalline and amorphous forms [17]. Recently Chen et al. were able to detect 0.37% amorphous content in mixtures of crystalline and amorphous lactose using the entire diffraction pattern in their analysis [18].

However, there are numerous potential errors associated with quantitative XRPD analysis which require consideration [19,20]. Thirty-three parameters, which can affect the accuracy of quantitative analysis using XRPD, were described by Hurst et al. [21]. These parameters can be grouped into three categories: instrumental factors, inherent properties of the analyte and parameters relating to sample preparation and mounting. Of the numerous sources of error apparent in quantitative XRPD studies, it appears

that the accuracy of quantification depends significantly on the minimisation of preferred orientation effects [13] which can affect peak intensity by up to 100% [21]. Some of the major sources of error associated with quantitative XRPD were examined by Suryanarayanan in his work involving carbamazepine [20,22], though rotation of the samples was not employed to reduce the errors from preferred orientation effects.

Here we have examined some of the major potential errors associated with quantitative XRPD analysis of mannitol polymorphs. Since the mannitol polymorphs have needle-like morphologies, preferred orientation effects were expected to be problematic with regard to the accuracy of quantitative data. These effects may be minimised by reducing the particle size [23], although sample grinding may induce polymorphic transformation [13] and disorder the crystal lattice [20]. Two particle size ranges were, therefore, investigated; below 125 and 125–500 μm, and the influence of sample rotation on preferred orientation errors was probed.

1.1. Theoretical background

Alexander and Klug [24] initially developed the theoretical basis for quantitative analysis used in XRPD, which has been subsequently been successfully used by Suryanarayanan [20,22,25]. Eq. (1) gives the basic relationship used in quantitative analyses involving PXRD [23,24].

$$Ii_J = \frac{Kx_J}{p_J \mu^*_m} \quad (1)$$

Ii_J is the intensity of line i (either from peak area or height) of the unknown component J, K is a constant, x_J represents the weight fraction of component J and p_J is the density of component J. The mass absorption coefficient of the matrix is depicted by μ^*_m. Here, mannitol mixtures contained the beta and delta polymorphs where delta is the 'unknown' component whilst beta is the matrix. Eq. (1) can, therefore, be rewritten to give Eq. (2) where Ii_δ is the intensity of line i of delta mannitol, x_δ and p_δ are the weight fraction and density of delta, respectively, and μ^*_β is the mass absorption coefficient of the beta polymorph.

$$Ii_\delta = \frac{Kx_\delta}{p_\delta \mu^*_\beta} \quad (2)$$

In a sample containing 100% delta mannitol, the intensity of line i (represented by $(Ii_\delta)_0$) can be determined using Eq. (3) where μ^*_δ is the mass absorption coefficient of the delta polymorph.

$$(Ii_\delta)_0 = \frac{K}{p_\delta \mu^*_\delta} \quad (3)$$

The ratio of intensities of line i in a delta mixture to the identical line in a sample containing only delta mannitol can, therefore, be determined using Eq. (4).

$$\frac{Ii_\delta}{(Ii_\delta)_0} = \frac{\mu^*_\delta x_\delta}{\mu^*_\beta} \quad (4)$$

Since beta and delta mannitol are polymorphs, their mass absorption coefficient values are the same which allows Eq. (4) to be adjusted to give Eq. (5).

$$\frac{Ii_\delta}{(Ii_\delta)_0} = x_\delta \quad (5)$$

Using Eq. (5), a plot of intensity ratio $(Ii_\delta/(Ii_\delta)_0)$ against the weight fraction of delta (x_δ) should give a straight line with a slope of 1.

2. Experimental section

2.1. Material preparation

Analar delta mannitol ($>99\%$, BDH Laboratory Supplies, UK) was used as obtained. β Mannitol was prepared by adding ~ 13 g of delta mannitol to 50 ml distilled water, stirring for 20 min at 50 °C before cooling to room temperature. The crystals formed were removed and allowed to dry naturally. Samples were lightly ground and sieved manually to give particle size ranges of below 125 and 125–500 μm.

2.2. Preparation of samples

About 0.5 g calibration mixtures of varying beta:delta mannitol composition were prepared for both particle size ranges. Samples were tumble mixed (Wad Turbula T2C, System Schatz, Switzerland) for 100 revolutions before use.

2.3. X-ray powder diffractometry

X-ray powder diffraction patterns of the samples were obtained using a Siemens D5000 powder diffractometer (Siemens, Karlsruhe, Germany) equipped with a scintillation counter detector and a divergent beam. This beam employed a Cu Kα source with a wavelength of 1.5418 Å containing 2 mm slits over the range of 9–25° 2θ with a step size of 0.05° 2θ and a count time of 1 s per step. The generator was set to 40 kV and 30 mA.

Samples were placed onto holders and rotation levels adjusted to obtain powder X-ray diffraction profiles from stationary and rotated samples (30 rpm). Data analysis was completed using GRAMS 32 version 5 software (Galactic Industries Corporation, USA).

2.4. Estimation of assay errors

Numerous potential assay errors associated with XRPD quantitative analysis were investigated, and are described in Table 1. For both particle size ranges, a single mixture of mid-calibration range was used to perform the estimation of assay errors using stationary and rotated sampling.

3. Results

3.1. Characterisation of the reference polymorphs

Qualitative analysis of the reference polymorphs was performed using FT-Raman spectroscopy and XRPD. Delta mannitol was certified as $>99\%$ pure and XRPD analysis of beta mannitol showed no evidence for contamination by other polymorphic forms when compared with literature diffraction profiles [26].

3.2. Determination of peak analysis parameters

Several methods have been employed to quantitatively examine XRPD peaks. Bugay et al. [8] used peak heights (in counts) against percentage weight as the calibration curve for quantification of cefepime·2HCl dihydrate in the monohydrate. Kontoyannis et al. [12] calculated the ratio of intensities of two selected diffraction lines in a mixture of gypsum and aragonite, which gave a linear relationship when, plotted against the corresponding molar fraction. In quantifying the degree of crystallinity, Clas et al. [16] selected six peaks and summated their peak areas to plot the total peak area against percentage crystallinity.

From the XRPD quantification work performed by Suryanarayanan [20,22], it is clear that diffraction line 'intensity' should use area under the curve of the peak and not peak height [25]; large variations in line shape resulting from differences in particle size can affect peak height whereas area would be invariant. Diffraction data from eight calibration samples were analysed by

Table 1
Some potential assay errors associated with quantitative analysis using PXRD

Error category	Measurement description
Day-to-day reproducibility	Variability in instrument response was investigated over a time period of 5 days. A single sample was placed in the instrument and a X-ray profile was recorded each day
Instrument reproducibility	Reproducibility of the instrument was investigated by acquiring six consecutive diffraction patterns of a single sample
Intra-day reproducibility	Variability of the instrument response during a typical working day was investigated by using a single sample and acquiring ten diffraction patterns over a 8 h period
Rotation rate	Effects of sample rotation were investigated by obtaining PXRD patterns of a single sample at rotation levels of 15, 30, 60 and 120 rpm
Sample mixing	To assess the variation due to sample mixing, the diffraction patterns of ten sub-samples were obtained from the whole sample mixture
Sample packing	Variations due to crystal orientation were assessed by re-packing the same sample ten times and acquiring a single diffraction profile after each packing
Sample positioning	Effects of variation in position of the sample holder within the instrument were examined by using a single sample and randomly repositioning the holder ten times

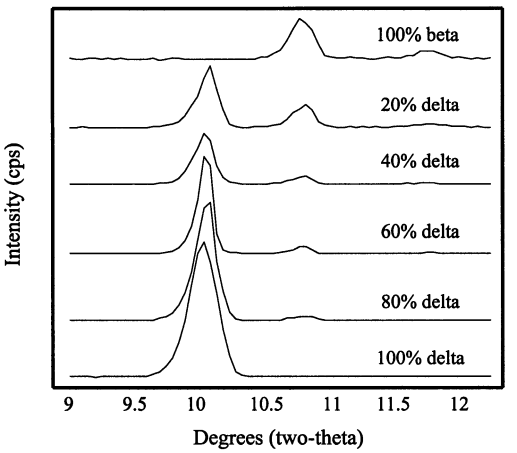

Fig. 1. XRPD profiles (9–12° 2θ region) of various compositions of beta and delta mannitol.

calculating both peak height and peak area; in agreement with literature expectations, data using peak areas was superior to that obtained from peak heights. Thus, the area under the delta peak situated at approximately 10° 2θ was subsequently used since this provided the strongest intensity and was unique to the delta form (Fig. 1). The 2-θ region of 9.5–10.4° provided sufficient angular range for the determination of peak area of delta and also allowed an adequate 2-θ region for the measurement of background area.

Several effects including lattice imperfections of the specimen may contribute to the scattering and diffraction of angles other than the Bragg reflections [27], therefore, the background intensity requires consideration and can be calculated from measurements on both sides of the peak which, ideally should equal the counts calculated for the peak area [20,23]. Unfortunately, in the case of beta and delta mannitol mixtures, a beta peak (situated approximately between 10.5 and 11° 2θ) restricts the angular range from which the background can be calculated, Fig. 1. The possible interference of this beta peak can be compensated for by calculating the background counts for the same number of steps as for those calculated for the delta peak [20]. This technique assumes that the background counts do not undergo any distinguishable change as a function of the scanning angle in the 2-θ region of interest [22].

Therefore, the number of steps was determined by dividing the selected theta range by the step size. The 2-θ range for the delta peak was 0.9° (9.5–10.4° 2θ), and the step size used in data collection was 0.05° thus the number of steps is 18. The background counts for the lower and higher values of two-theta were calculated, permitting the same number of steps to be integrated for both the delta peak and the background. The calculated area of the background was subtracted from the peak area to give a net peak area (Ii_δ) which represents the peak area of delta in a mixture containing various proportions of beta and delta mannitol. Ii_δ is divided by the net peak area of a sample containing only delta mannitol ($(Ii_\delta)_0$) and the resulting ratio is then plotted against the mole fraction of the delta component to produce a correlation curve.

3.3. Preparation of the correlation curve

The resulting mean ratio values $(Ii_\delta/(Ii_\delta)_0)$ for each of the correlation samples were multiplied by 100 to convert the values into percentage calculated delta concentration. The calculated delta concentrations were plotted against actual delta concentrations for each of the four sample groups (rotation/ < 125 μm; rotation/125–500 μm; no rotation/ < 125 μm; no rotation/125–500 μm) (Fig. 2).

3.4. Evaluation of limit of detection and limit of quantitation

The LOD of the quantitative method was calculated using Eq. (6) where S_m is the minimum distinguishable analytical signal, M_{bl} is the mean blank signal, k is a multiple (3 in this case as three measurements were recorded for each sample) and s_{bl} is the standard deviation of the blank signal [28].

$$S_m = M_{bl} + ks_{bl} \quad (6)$$

The relationship between the measured signal (S) and the concentration of the analyte (C) is shown in Eq. (7) where m is the slope of the calibration curve and S_{bl} is the instrumental signal for the blank sample.

$$S = mC + S_{bl} \quad (7)$$

Eq. (7) can be adapted to calculate the minimum concentration at which a measurable signal (S_m) is observed to give Eq. (8) where C_m represents the LOD.

$$S_m = mC_m + M_{bl} \quad (8)$$

The LOD can be calculated directly by rewriting Eq. (8) to give Eq. (9).

$$\text{LOD} = C_m = \frac{(S_m - M_{bl})}{m} \quad (9)$$

The LOQ is given as ten standard deviations of the blank signal (Eq. (10)).

$$\text{LOQ} = 10 \times s_{bl} \quad (10)$$

The C_m (LOD) and LOQ values for each of the four sample groups are given in Table 2.

3.5. Estimation of sources of error

The relative standard deviation (R.S.D.) associated with each error category was calculated using Eq. (11) where S.D. represents the standard deviation of the measurement and m is the mean $Ii_\delta/(Ii_\delta)_0$ value. The R.S.D. value for each error category could then be compared for each of the four sample groups (Table 3).

$$\text{R.S.D.} = \frac{\text{S.D.}}{m} \times 100 \quad (11)$$

4. Discussion

4.1. Quantitation of delta mannitol

4.1.1. Effects of rotation

For each correlation curve the line of best-fit was selected and correlation coefficients calculated (R^2) (Fig. 2). The R^2 values ranged from 0.957 to 0.983, which are somewhat lower than values expected for correlation curves [29]. Data from the rotated samples of both particle size

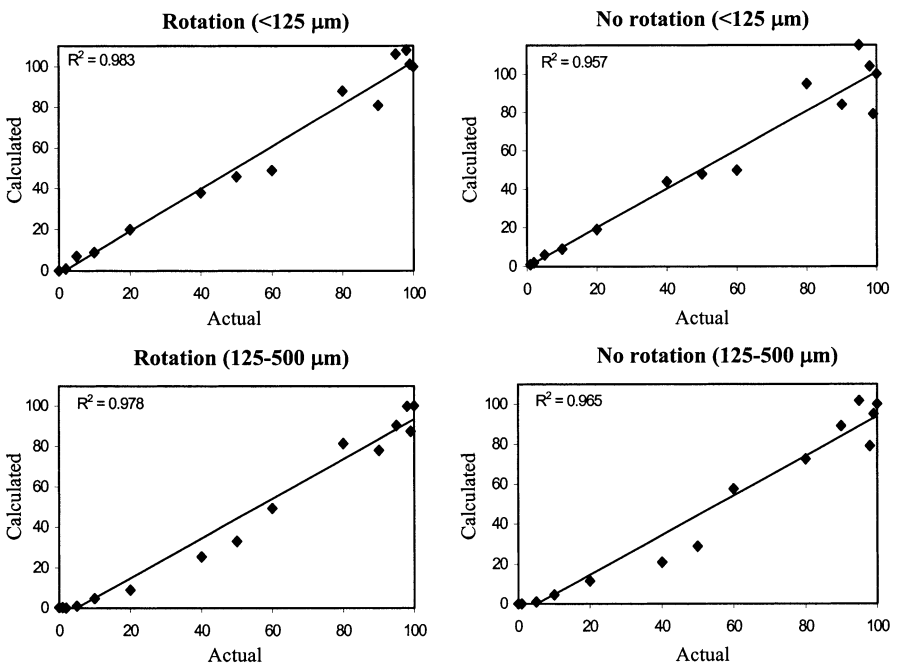

Fig. 2. Correlation curves (calculated delta concentration vs. actual delta concentration in percentage) of the < 125 and 125–500 μm samples analysed with alteration of sample rotation.

Table 2
Mean calculated delta concentrations, LOD and LOQ (%) calculated from PXRD patterns with S.D. ($n = 3$) in parentheses.

Actual percentage of delta	<125 μm Particles		125-500 μm Particles	
	Rotation of samples	No rotation of samples	Rotation of samples	No rotation of samples
0	0.05 (0.4)	−0.21 (0.12)	0.14 (0.7)	−0.04 (0.2)
0.5	−0.14 (0.1)	−0.14 (0.26)	−0.14 (0.14)	−0.6 (0.9)
1	−0.7 (1.1)	0.6 (1.2)	0.19 (1.6)	0.02 (0.2)
2	1.4 (1.4)	1.6 (0.8)	0.04 (1.0)	−0.2 (0.5)
5	6.8 (1.7)	6.4 (1.4)	0.9 (0.01)	1.0 (0.4)
10	8.5 (1.0)	8.5 (1.8)	4.8 (2.1)	4.5 (0.6)
20	19.8 (1.0)	19.4 (1.7)	9.0 (2.3)	11.5 (5.2)
40	37.6 (5.6)	44.2 (11.7)	25.6 (1.4)	20.9 (5.9)
50	45.8 (9.1)	48.4 (5.6)	33.0 (4.4)	28.9 (9.1)
60	49.3 (8.7)	50.3 (10.1)	49.3 (10.2)	57.5 (4.8)
80	88.2 (5.9)	94.9 (5.6)	81.3 (5.2)	72.5 (7.3)
90	81.2 (9.7)	84.0 (19.0)	78.2 (13.8)	88.9 (9.2)
95	106.4 (10.4)	115.2 (24.4)	90.4 (3.4)	101.7 (21.4)
98	107.7 (19.9)	103.5 (27.9)	99.7 (14.3)	78.8 (3.0)
99	100.5 (15.8)	78.7 (8.1)	87.5 (9.1)	94.9 (23.0)
100	100.0 (17.0)	100.0 (14.3)	100.0 (22.0)	100.0 (19.2)
LOD	1	0.3	2.1	0.6
LOQ	3.6	1.2	7	1.8

ranges gave R^2 values higher than their non-rotated counterparts suggesting that sample rotation improves the correlation between the actual and measured amount of delta present. For the most part, the mean calculated delta concentrations of the <125 μm samples showed close agreement regardless of rotation (Table 2). The standard deviation associated with the mean concentration was however, generally greater for the non-rotated samples. This indicates that measurements more representative of the overall sample mixture were obtained through sample rotation.

4.1.2. Particle size effects

The mean calculated delta concentration of the larger particle size range exhibited greater variation between the rotated and non-rotated mixtures with half of the samples showing approximately 5–20% variation. This provides strong evidence for the existence of preferred orientation effects with the 125–500 μm particle size range since a change of more than 10% in the intensity of a peak when the sample is rotated is a potential indicator of preferred orientation effects [21].

4.1.3. Limits of detection and quantitation

The LOD value obtained for the rotated <125 μm sample in this study is comparable to those recorded by other workers [8,17] although the corresponding LOQ value is higher. From the data in Table 2 it can be seen that reducing the particle size from 125 to 500 μm to below 125 μm halved the calculated LOD and LOQ values for both the rotated and non-rotated samples. This indicates that the detection and quantitation limit for the method can be improved by reducing the particle size range of the samples.

The data in Table 2 also indicate that the non-rotated samples for both particle size ranges give the lowest LOD and LOQ values despite exhibiting the lowest correlation coefficients of all the correlation curves (Fig. 2). The low LOD and LOQ values of the non-rotated mixtures may be attributed to negative mean $Ii_\delta/(Ii_\delta)_0$ values. The LOD is determined from calculations using the blank sample (only beta mannitol present) and examination of the appropriate data revealed greater peak area values for the surrounding background than the actual region used for delta peak area measurement; preferred orientation of

the needle crystals may account for this observation.

From the lower LOD and LOQ values presented in Table 2 it would initially appear that not rotating the sample improves assay sensitivity. However, the value of this quantitative assay can not be based solely on the LOD and LOQ values because the calibration data generally indicate that less variation is observed with the mean $Ii_{\delta}/(Ii_{\delta})_0$ values obtained from the rotated < 125 μm rather than the corresponding non-rotated samples. The greatest correlation between the actual and calculated concentration values was for the calibration curve plotted using the rotated < 125 μm samples. Therefore, the LOD and LOQ data presented in Table 2 may appear misleading and the accuracy and precision of all the correlation data must be considered when determining the analytical value of this technique for quantitative purposes.

5. Estimation of assay errors

Instrument reproducibility was determined by recording six consecutive measurements of a sample without disturbance. Variation arising through instrument reproducibility was up to 2%, with the < 125 μm rotated samples showing the lowest R.S.D. of 1.1%. The non-rotated 125–500 μm samples exhibited the greatest R.S.D. (2%) which was surprising since the error category involved recording six consecutive measurements without sample disturbance. The data in Table 3 indicates that sample rotation reduces the variation associated with instrument reproducibility.

Day-to-day reproducibility was examined by collecting daily diffraction patterns of a single sample for a period of 5 days. The variation observed with samples with a particle size range below 125 μm on a day-to-day basis was in the region of 5%. For the 125–500 μm mixtures, the variation recorded was approximately 16 and 31% for the rotated and non-rotated samples, respectively; this difference in variation with particle size indicates the presence of preferred orientation effects with the larger particles. These errors appear excessive when compared with those from intra-day variation. However, it should be borne in mind that the day-to-day error for which the sample was removed daily from the instrument is a composite including variability resulting from sample re-positioning and possibly from sample disturbance on re-analysis.

Sample positioning effects were assessed by randomly repositioning the sample holder ten times. Rotation of the < 125 μm samples appeared to have little effect on the variation arising from sample positioning (Table 3), but the significant difference in R.S.D. values of the rotated and non-rotated 125–500 μm samples suggests that preferred orientation effects occur with these larger particles. The variation associated with positioning of the 125–500 μm sample was reduced (approximately 5-fold) through sample rotation. Thus, errors induced by preferred orientation effects can be reduced through rotation.

Table 3
R.S.D. (%) of results obtained for each of the potential error categories investigated using PXRD

Error category	<125 μm Particles		125–500 μm Particles	
	Rotation[a]	No rotation	Rotation[a]	No rotation
Day-to-day reproducibility	4.3	5	16.1	30.8
Instrument reproducibility	1.1	1.4	1.3	2.0
Intra-day reproducibility	1.5	2.1	2.0	1.8[b]
Sample mixing	19.7	33.4	21.3	26.4
Sample packing	19.9	16.7[b]	23.8	30.0
Sample positioning	6.1	6.0	3.0	14.5[a]

R.S.D. values associated with: a, mean of nine samples; b, mean of eight samples.
[a] Rotation rate of 30 rpm.

Sample packing effects were investigated by re-packing a single sample ten times, recording a diffraction pattern after each preparation. The < 125 μm samples exhibit only a minor difference in the R.S.D. values between the rotated and non-rotated samples. In comparison, the R.S.D. values for the rotated and non-rotated 125–500 μm samples are larger indicating that greater variation due to sample packing is observed for the bigger particle size range. Re-packing the same sample results in a variation of 30% for the non-rotated 125–500 μm particle size range samples which was reduced to 24% for the corresponding non-rotated 125–500 μm samples.

Sample mixing effects were assessed by collecting diffraction patterns of ten sub-samples of a single sample mixture, which resulted in R.S.D.'s between 19 and 34%. From the data shown in Table 3 it can be seen that rotating the samples reduced the variation associated with sample mixing for both particle size ranges.

Intra-day reproducibility was investigated by recording ten diffraction patterns of a single samples over a time period of 8 h. The investigation of intra-day reproducibility resulted in variations between ~ 1 and 2% for all four sample groups. Relatively small variation for intra-day reproducibility was expected since the same mixture was measured across an 8 h period without sample disturbance. From the data in Table 3 it can be demonstrated that consistent instrumental response across time periods of 1 h (instrument reproducibility) and 8 h (intra-day reproducibility) was observed.

The effect of varying rotation rate on profile quality was examined by obtaining diffraction patterns from a single sample rotated at 15, 30, 60 and 120 rpm. Measurements were collected using a scan rate of 1 s per 0.05° step. One complete rotation of the sample would have taken approximately 4 s for the 15 rpm level, 2 s for 30 rpm, 1 s for 60 rpm and 0.5 s for 120 rpm. Thus it might have been expected for the pattern of the sample collected using 120 rpm to be more representative of the overall mixture since relatively more of the sample is involved in the measurement for each two-theta step taken than the other rotation rates. However, in this study, little variation was observed between the calculated delta percentages for each rotation rate. This indicates that although sample rotation appears beneficial in reducing the errors associated with preferred orientation, the rate of rotation appears to be a less critical factor and that any of the rotation rates adopted in this study could be used for quantitative analysis.

Generally, the non-rotated 125–500 μm samples exhibited the greatest R.S.D. values for the majority of assay errors investigated. Rotation of these samples reduced the R.S.D. values of all the errors other than intra-day reproducibility, which was essentially invariant.

From the potential errors investigated in this study, control of parameters such as sample packing and mixing appear critical to the accuracy of the data obtained. Generally, parameters involving the response of the instrument with no sample disturbance (instrument and intra-day reproducibility) gave relatively small R.S.D. values (around 2%) indicating good reproducibility of the technique. Similar observations were seen in the quantitative analysis of mannitol polymorphs using FT-Raman spectroscopy where the largest sources of variation could again be attributed to the sample packing and mixing categories. Good reproducibility (relatively small R.S.D. values) was also obtained for the instrument and intra-day reproducibility error categories [10]. The R.S.D. value recorded for the < 125 μm sample mixing error was 3% for the spectroscopic study compared with 19–33% obtained for this work. The former variation was attributed to inhomogeneous mixing of the particles, which resulted in non-representative measurements since relatively small volumes of sample were analysed per FT-Raman spectrum recorded. However, for XRPD analysis, sampling involved the majority of the 0.5 g calibration mixture, which should have allowed a more representative measurement of the sample. Thus it is likely that preferred orientation effects rather than inhomogeneous mixing of the particles are responsible for the larger variation observed.

The estimation of assay errors performed by Bugay et al. [8] used particles of 125–590 μm and since no mention of sample rotation was made,

their results could be compared with the data obtained in Table 3 for the non-rotated 125–500 μm samples. For each of the error categories listed in Table 3 (with the exception of intra-day reproducibility) Bugay et al. [8] observed a variation of 5.3–7.6%, significantly lower than the variation observed for the day-to-day reproducibility, sample-positioning, -packing and -mixing categories in this study. Interestingly, the cefepime·2HCl samples analysed by Bugay et al. [8] included plate-like crystals, which are less prone to preferred orientation effects as is the case for mannitol polymorphs than crystals with needle-like morphologies, as is the case for mannitol polymorphs. It would be of benefit to determine the errors associated with XRPD quantitative analysis from materials with a range of crystal habits in order to probe the utility of the method for diverse particulate systems.

6. Conclusions

The effects of particle size and sample rotation on XRPD quantitative analysis of mannitol polymorphs were probed. Rotating samples and reducing particle size halved the LOD and LOQ values to 1 and 3.6%, respectively.

Some of the major potential assay errors were examined which provided the bulk of variation to the data. Instrumental accuracy and precision contributed typically $< 2\%$ variation to all samples with sample packing and mixing errors contributing the greatest variation to the data. Preferred orientation of the particles could explain the large variations seen with the majority of the error categories. In conclusion, reducing the particle size to < 125 μm improved assay accuracy, as did rotating the sample for most of the errors examined. Thus, if grinding a polymorphic system to reduce particle size is problematic with regard to stability, sample rotation offers an alternative approach for assay error reduction.

The present study demonstrates that polymorphs exhibiting very similar XRPD profiles can be successfully quantified using this technique but attention must be given to the size of the crystals involved. Generally, a reduction in particle size improved the limits of detection and quantitation and associated assay errors.

The main limitation of this method with regard to the quantification of mannitol is likely to be the morphology of the crystals involved. The needle-like particles are prone to preferred orientation, which has been shown to significantly influence the data in this study. The assay may have been complicated by the fact that both components have needle-like habits. Preferred orientation effects were reduced by rotating the samples, which could serve to improve the accuracy of future quantitative studies involving XRPD.

From this work and studies performed by other workers [8], crystal morphology appears to influence the degree of variation observed with quantitative XRPD errors. Thus, it would be of great interest to study the effect of particle morphology on the accuracy of quantitative analysis using XRPD. From this, workers could assess the suitability of XRPD for quantitative analysis depending on the crystal morphology of their material.

Acknowledgements

The authors would like to thank Merck, Sharp and Dohme Research Laboratories and the EPSRC for financial support.

References

[1] S.R. Vippagunta, H.G. Brittain, D.J.W. Grant, Adv. Drug Deliv. Rev. 48 (2001) 3–26.
[2] S. Byrn, R.R. Pfeiffer, M. Ganey, C. Hoiberg, G. Poochikian, Pharm. Res. 12 (1995) 945–954.
[3] K. Knapman, Mod. Drug Disc. 3 (2000) 53–57.
[4] N.A. Armstrong, G.E. Reier, in: A.H. Kribbe (Ed.), Handbook of Pharmaceutical Excipients, Pharmaceutical Press, London, 2000, pp. 324–328.
[5] SPI Polyols. http://www.spipolyols.com/polyols/gen_sht.html (1999).
[6] A.D. Patel, P.E. Luner, M.S. Kemper, Int. J. Pharm. 206 (2000) 63–74.
[7] P.E. Lunar, S. Majuru, J.J. Seyer, M.S. Kemper, Pharm. Dev. Technol. 5 (2000) 231–246.
[8] D.E. Bugay, A.W. Newman, W.P. Findlay, J. Pharm. Biomed. Anal. 15 (1996) 49–61.
[9] L.S. Taylor, G. Zografi, Pharm. Res. 15 (1998) 755–761.

[10] S.N. Campbell Roberts, A.C. Williams, I.M. Grimsey, S.W. Booth, J. Pharm. Biomed. Anal. (2002), in press.
[11] C.G. Kontoyannis, N.C.H. Bouropoulos, P.G. Koutsoukos, Appl. Spectrosc. 51 (1997) 64–67.
[12] C.G. Kontoyannis, M.G. Orkoula, P.G. Koutsoukos, Analyst 122 (1997) 33–38.
[13] G.A. Stephenson, R.A. Forbes, S.M. Reutzel-Edens, Adv. Drug Deliv. Rev. 48 (2001) 67–90.
[14] P. Gao, Pharm. Res. 13 (1996) 1095–1104.
[15] R.S. Chao, K.C. Vail, Pharm. Res. 4 (1987) 429–432.
[16] S.-D. Clas, R. Faizer, R.E. O'Connor, E.B. Vadas, Int. J. Pharm. 121 (1995) 73–79.
[17] R. Surana, R. Suryanarayanan, Powder Diff. 15 (2000) 2–6.
[18] X. Chen, S. Bates, K.R. Morris, J. Pharm. Biomed. Anal. 15 (1997) 687–696.
[19] S. Agatonovic-Kustrin, V. Wu, T. Rades, D. Saville, I.G. Tucker, Int. J. Pharm. 184 (1999) 107–114.
[20] R. Suryanarayanan, Powder Diff. 5 (1990) 155–159.
[21] V.J. Hurst, P.A. Schroeder, R.W. Styron, Anal. Chim. Acta 337 (1997) 233–252.
[22] R. Suryanarayanan, Pharm. Res. 6 (1989) 1017–1024.
[23] H.P. Klug, L. Alexander, X-ray Diffraction Procedures for Polycrystalline and Amorphous Materials, Wiley, New York, 1974.
[24] L. Alexander, H.P. Klug, Anal. Chem. 20 (1948) 886–889.
[25] R. Suryanarayanan, Int. J. Pharm. 77 (1991) 287–295.
[26] A. Burger, J.-O. Henck, S. Hetz, J.M. Rollinger, A.A. Weissnicht, H. Stottner, J. Pharm. Sci. 89 (2000) 457–468.
[27] B.D. Cullity, Elements of X-ray Diffraction, Addison-Wesley, Massachusetts, 1978.
[28] D.A. Skoog, F.J. Holler, T.A. Nieman, Principles of Instrumental Analysis, Saunders College Publishing, Philadelphia, 1998.
[29] J.C. Miller, J.N. Miller, Statistics for Analytical Chemistry, Ellis Horwood, UK, Chichester, 1994.